

Quantum interference by a nonlocal double slit

E. J. S. Fonseca,¹ P. H. Souto Ribeiro,² S. Pádua,¹ and C. H. Monken^{1,*}

¹*Departamento de Física, Universidade Federal de Minas Gerais, Caixa Postal 702, Belo Horizonte, MG 30123-970, Brazil*

²*Instituto de Física, Universidade Federal do Rio de Janeiro, Caixa Postal 68.528, Rio de Janeiro 22945-970, RJ, Brazil*

(Received 18 November 1998)

We report an interference experiment in which photon pairs generated by spontaneous parametric down-conversion produce a Young-type fourth-order interference pattern after being scattered by two different and spatially separated apertures, whose superposition defines a double slit. The experiment is compared with previous ones based on parametric down-conversion, and its nonlocal nature is discussed. A theoretical explanation is also provided. [S1050-2947(99)06507-5]

PACS number(s): 42.50.Ar, 03.65.Bz, 42.50.Dv

I. INTRODUCTION

Entanglement is one of the most striking features of quantum mechanics. It is the basis of the exciting new fields of quantum computing, quantum cryptography [1], and teleportation [2,3]. Some nonlocal [4] aspects of entanglement have been explored in a variety of experimental situations in quantum optics, from which one can cite the Einstein-Podolsky-Rosen experiments [5–10], two-photon optics [11], transverse interference effects [12–14], and conditional interference [15]. In the latter three, the momentum entanglement causes the fourth-order spatial correlation function of the electromagnetic field to be dependent on the relative transversal position of two spatially separated photodetectors. Recently, Monken, Souto Ribeiro, and Pádua [14] showed that the two-photon optics [11] can be understood as a transfer of angular spectrum from the pump beam to the two-photon field generated by the process of spontaneous parametric down-conversion in a thin crystal. The transfer of angular spectrum provides an easy way to control the fourth-order spatial correlation of that field.

In this paper we discuss an interesting consequence of momentum entanglement: the ability of a two-photon field to mimic the scattering by a double slit, when this field is scattered by two spatially separated apertures, none of them being a double slit. Rather, the superposition of the two apertures do define a double slit, which determines the shape of the two-point fourth-order transverse spatial correlation function. The situation is represented in Fig. 1, where the entangled two-photon field is generated by spontaneous parametric down-conversion (SPDC).

An extension of the theory developed in Ref. [14] is shown to be able to describe our experimental results. We also compare the experiment with previous ones [7–10,12,13,16–20], emphasizing the nonlocal character of the interference effects.

II. EXPERIMENT

The experimental setup is represented in Fig. 2. The down-converter was a 7-mm-long BBO crystal, whose opti-

cal axis lies in the horizontal plane, pumped by an Argon laser operating at 351.1 nm, TEM₀₀ power stabilized mode, with an output power of approximately 50 mW. The crystal was cut for type II phase matching at $\lambda_1 = \lambda_2 = 702$ nm, with output angles of approximately 4° , with respect to the pumping direction. Detectors D_1 and D_2 were avalanche photodiodes operating in the photon counting mode, placed at 100 cm from the crystal. In front of each detector there was an arrangement composed by a slit of $0.1 \text{ mm} \times 5 \text{ mm}$ horizontally aligned, followed by a microscope objective focused on the active area. D_1 and D_2 were connected to single and coincidence counters with a resolving time of 10 ns. The apertures A_1 and A_2 were chosen as indicated in Fig. 1, where A_1 was a $0.4\text{-mm} \times 10\text{-mm}$ single slit, and A_2 was a 0.2-mm-diameter wire. Both A_1 and A_2 were placed at $z_A = 48$ cm from the crystal. A convergent lens L of 50-cm focal length was placed in the pump beam, so that the beam waist w_0 was located at 48 cm from the crystal, right on the plane of the apertures. The measured beam diameter at this position was $2w_0 = 0.15$ mm.

Coincidence rates, which are proportional to the fourth-order correlation function, were recorded as functions of detectors' D_1 and D_2 vertical positions. Single count rates were also recorded.

III. THEORY

In order to account for the effect of the apertures in the quantized field, let us start from the classical solution. Sup-

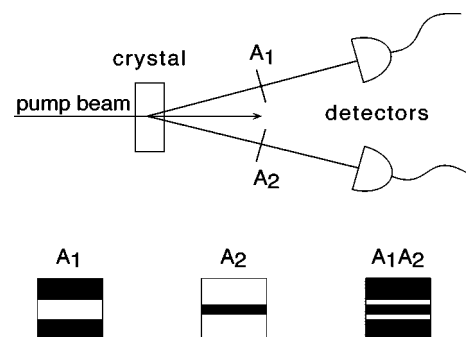


FIG. 1. Top: basic arrangement for the experiment. Bottom: detail of the apertures.

*Author to whom correspondence should be addressed. Electronic address: monken@fisica.ufmg.br

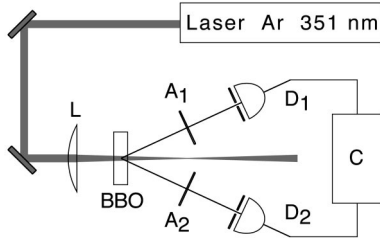


FIG. 2. Experimental setup.

pose that a monochromatic field $E(\mathbf{r})$, propagating around the z direction, is known at the plane $z=0$. In terms of its spatial Fourier components, $E(\mathbf{r})$ can be written as

$$E(\boldsymbol{\rho}, 0) = \int d\mathbf{q} A(\mathbf{q}) e^{i\mathbf{q} \cdot \boldsymbol{\rho}}, \quad (1)$$

where $\boldsymbol{\rho}$ and \mathbf{q} are the transverse components of \mathbf{r} and \mathbf{k} , respectively. After being scattered by an aperture $A(\boldsymbol{\rho})$ placed on the plane $z=z_A$, the far field in the paraxial approximation is [21]

$$E(\boldsymbol{\rho}, z) = e^{ikz} \int d\mathbf{q} \int d\mathbf{q}' A(\mathbf{q}') T(\mathbf{q} - \mathbf{q}') \times \exp\left\{i\left[\mathbf{q} \cdot \boldsymbol{\rho} - \frac{q^2}{2k}(z - z_A) - \frac{q'^2}{2k}z_A\right]\right\}, \quad (2)$$

where $T(\mathbf{q})$ is the Fourier transform of $A(\boldsymbol{\rho})$. Now, replacing $E(\mathbf{r})$ and $A(\mathbf{q})$ by quantum mechanical operators, we arrive at the following operator for the scattered far field:

$$E^{(+)}(\boldsymbol{\rho}, z) = e^{ikz} \int d\mathbf{q} \int d\mathbf{q}' a(\mathbf{q}') T(\mathbf{q} - \mathbf{q}') \times \exp\left\{i\left[\mathbf{q} \cdot \boldsymbol{\rho} - \frac{q^2}{2k}(z - z_A) - \frac{q'^2}{2k}z_A\right]\right\}. \quad (3)$$

For a thin nonlinear crystal centered at the origin and pumped along the z direction, the state generated by SPDC in the monochromatic and paraxial approximations can be represented by [14]

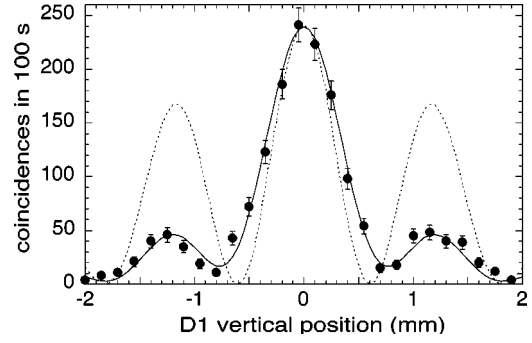
$$|\psi\rangle = |\text{vac}\rangle + \text{const.} \int d\mathbf{q}_1 \int d\mathbf{q}_2 v(\mathbf{q}_1 + \mathbf{q}_2) |1; \mathbf{q}_1\rangle |1; \mathbf{q}_2\rangle, \quad (4)$$

where $|1; \mathbf{q}\rangle$ represents a one-photon state with transverse wave vector component \mathbf{q} , and $v(\mathbf{q})$ is the angular spectrum of the pump field at $z=0$.

Combining expressions (3) and (4) we can calculate the fourth-order correlation function

$$G_{12}^{(2,2)}(\mathbf{r}_1, \mathbf{r}_2) = \langle E_2^{(-)}(\boldsymbol{\rho}_2, z_2) E_1^{(-)}(\boldsymbol{\rho}_1, z_1) \times E_1^{(+)}(\boldsymbol{\rho}_1, z_1) E_2^{(+)}(\boldsymbol{\rho}_2, z_2) \rangle, \quad (5)$$

when the apertures A_1 and A_2 are placed at z_{A1} and z_{A2} . After some algebra we have

FIG. 3. Coincidence counts when detector D_1 is moved. Solid line: numerical solution of Eq. (9). Dotted line: solution of Eq. (8).

$$G_{12}^{(2,2)}(\mathbf{r}_1, \mathbf{r}_2) = |g(\mathbf{r}_1, \mathbf{r}_2)|^2, \quad (6)$$

where

$$g(\mathbf{r}_1, \mathbf{r}_2) = \text{const} \int d\xi \int d\eta A_1(\xi) A_2(\eta) \mathcal{W} \times \left(\frac{\xi}{2} + \frac{\eta}{2}, z_A\right) \exp\left[i\frac{k}{2}\left(\frac{|\boldsymbol{\rho}_1 - \xi|^2}{z_1 - z_A} + \frac{|\boldsymbol{\rho}_2 - \eta|^2}{z_2 - z_A}\right)\right] \exp\left(ik\frac{|\xi - \eta|^2}{4z_A}\right), \quad (7)$$

where $\mathcal{W}(\boldsymbol{\rho}, z_A)$ is the transverse profile of the pump field at $z=z_A$. In order to simplify the calculations, the following conditions were assumed: $k_1=k_2=k$, $k_1+k_2 \approx k_p$ (collinear or quasicollinear phase matching), $z_{A1}=z_{A2}=z_A$.

Now, if we consider the particular case of a pump beam focused at $z=z_A$, so that $\mathcal{W}(\boldsymbol{\rho}, z_A)$ can be approximated by a delta function, $g(\mathbf{r}_1, \mathbf{r}_2)$ becomes

$$g(\mathbf{r}_1, \mathbf{r}_2) = \text{const.} \int d\xi A_1(\xi) A_2(-\xi) \exp\left(ik\frac{\xi^2}{4z_A}\right) \times \exp\left[ik\frac{\left|\frac{1}{2}(\boldsymbol{\rho}_1 - \boldsymbol{\rho}_2) - \xi\right|^2}{z_d - z_A}\right]. \quad (8)$$

Again, for simplicity, we have considered $z_1=z_2=z_d$. The above expression describes the propagation of light from an effective aperture defined by $A_1(\xi)A_2(-\xi)$ at $z=z_A$ to the detection plane ($z=z_d$), in the paraxial approximation, with wave number $2k$. When $z_d - z_A$ is large enough, this propagation leads to the diffraction pattern of the effective aperture as a function of the transverse coordinate $\frac{1}{2}(\boldsymbol{\rho}_1 - \boldsymbol{\rho}_2)$. In practice, however, the dimensions of the apertures A_1 and A_2 are usually of the order of a few hundred μm , so the focused pump beam profile can hardly be approximated by a delta function. A direct (numerical) solution of expression (7) is then required, as discussed in Sec. IV.

IV. RESULTS AND DISCUSSION

Figure 3 shows the results of coincidence counts in sampling times of 100 s, when detector D_1 is moved in steps of 0.15 mm, while detector D_2 is held at $y_2=0$. Figure 4 shows

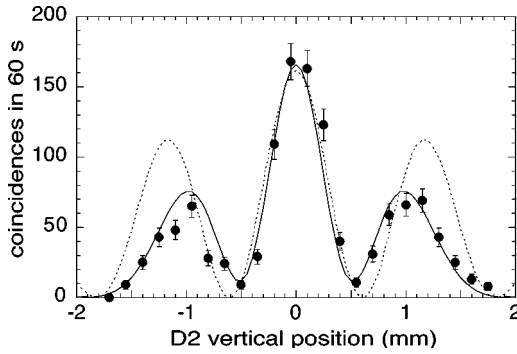


FIG. 4. Coincidence counts when detector D_2 is moved. Solid line: numerical solution of Eq. (9). Dotted line: solution of Eq. (8).

the same kind of measurement when D_2 is moved while D_1 is held at $y_1 = 0$. In both cases, Young-type interference patterns are readily identified, although they do not refer to the same effective aperture. This asymmetry is due to the finite diameter of the pump beam at $z = z_A$, which is of the same order of magnitude as the dimensions of the apertures. A numerical solution of expression (6) in the one-dimensional case was carried out, that is,

$$G_{12}^{(2,2)}(y_1, y_2, z_d) = \text{const} \left| \int d\xi \int d\eta A_1(\xi) A_2(\eta) \right. \\ \times \exp \left[- \left(\frac{\xi + \eta}{2w_0} \right)^2 + \frac{ik}{4z_A} (\xi - \eta)^2 \right] \\ \left. \times \exp \left\{ ik \left[\frac{(y_1 - \xi)^2 + (y_2 - \eta)^2}{2(z_d - z_A)} \right] \right\} \right|^2, \quad (9)$$

setting all parameters to the corresponding experimental values. The solid lines in Figs. 3 and 4 are solutions of expression (9), normalized to the number of coincidences, with no additional fitting, whereas the dotted lines represent the solution of expression (8), the limiting case. Figure 5 shows the single counts of both detectors, which are expected from apertures A_1 and A_2 , illuminated by an extended source (the interaction region in the crystal).

The above results show that double-slit interference patterns are observed in the coincidence counting rate, even though individual *signal* and *idler* intensity profiles have nothing to do with double-slit patterns. Previous experiments with double-slits and coincidence detection are based on the passage of one of the beams (*signal* [12], *idler* [13], or *pump* [14]) through a *localized* double slit. In other interference experiments, with twin photons and coincidence detection, beams were also passed through *localized* interferometers, such as a Mach-Zehnder [16] or a Michelson [18,19].

In those experiments where localized interferometers were used, it is possible to provide *local* interpretations. For example, when intensity interference fringes do not show up and coincidence interference fringes do, we can think of them as being a result of a spectral filtering process due to the coincidence measurements. This is a consequence of the fact that when SPDC light passes through a local interferom-

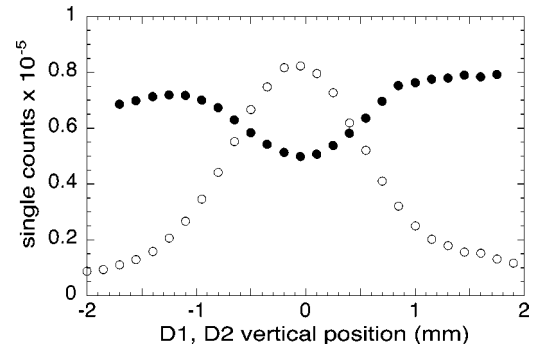


FIG. 5. D_1 (\circ) and D_2 (\bullet) single counts as functions of each detector position when the other is kept at zero.

eter and the intensity pattern produced does not present fringes, we can regard this pattern as a continuous superposition of interference patterns displaced in space or time, resulting in fringes with extremely low visibility. When coincidence measurements are performed, a subensemble within that continuum of patterns is selected [12].

In the present experiment with nonlocal double slits, this kind of *local* interpretation is not possible, since no Young interference patterns can be associated with the intensity distributions in neither *signal* nor *idler* beams. It must be noted that we are not claiming that our experiment shows nonlocal interference effects and previous ones do not. The above mentioned filtering process, due to coincidence detection between two spatially separated detectors, may exhibit a nonlocal character. In those cases, however, the nonlocality cannot be associated with the mere appearance of interference fringes, but rather to their high visibility. In our case, it is clear that the nonlocal character of the interference process is explicit.

We find an analogy between the present experiment and two others. The first one was introduced by Rarity and Tapster [20]. In that case, it is possible to identify a nonlocal Mach-Zehnder in which one of the beam splitters is placed in the *idler* beam and the other one is placed in the *signal*. The second experiment is the usual Bell state polarization interferometer [6], where each of the polarization analyzers can be viewed as part of a nonlocal interferometer in the spin space, since the coincidence pattern depends on the relative angle between the analyzer's axis. In both cases [6,20], nonlocality is quantitatively evaluated by means of a Bell inequality, which is violated.

A Bell-type inequality for position variables was derived by Ou [22], but it does not apply to our experiment. Even though we cannot evaluate it quantitatively, our experimental results suggest that strong nonlocal correlations are present.

In conclusion, we have presented a quantum interference experiment using a nonlocal double slit. We have presented a quantum theory in good agreement with experimental results. We have also pointed out the connections between our experiment and other ones that violate Bell inequalities.

ACKNOWLEDGMENTS

The authors acknowledge financial support from the Brazilian agencies CNPq, FINEP, PRONEX, and FAPEMIG.

- [1] C. H. Bennett, *Phys. Today* **48** (10), 24 (1995).
- [2] D. Bouwmeester *et al.*, *Nature (London)* **390**, 575 (1997).
- [3] D. Boschi *et al.*, *Phys. Rev. Lett.* **80**, 1121 (1998).
- [4] The expression “nonlocal” is too general in this context. Rigorously speaking, we should use the more appropriate expression “nonlocal-realistic.” However, for the sake of brevity, many workers refer to “nonlocal-realistic” as “nonlocal.” In this paper we adopt this common practice.
- [5] A. Einstein, B. Podolsky, and N. Rosen, *Phys. Rev.* **47**, 777 (1935).
- [6] A. Aspect, P. Grangier, and G. Roger, *Phys. Rev. Lett.* **47**, 460 (1981).
- [7] Z. Y. Ou and L. Mandel, *Phys. Rev. Lett.* **61**, 50 (1988).
- [8] Y. H. Shih and C. O. Alley, *Phys. Rev. Lett.* **61**, 2921 (1988).
- [9] J. R. Torgerson, D. Branning, C. H. Monken, and L. Mandel, *Phys. Lett. A* **204**, 323 (1995).
- [10] J. R. Torgerson, D. Branning, C. H. Monken, and L. Mandel, *Phys. Rev. A* **51**, 4400 (1995).
- [11] T. B. Pittman *et al.*, *Phys. Rev. A* **53**, 2804 (1996).
- [12] P. H. S. Ribeiro, S. Pádua, J. C. M. da Silva, and G. A. Barbosa, *Phys. Rev. A* **49**, 4176 (1994).
- [13] D. V. Strekalov, A. V. Sergienko, D. N. Klyshko, and Y. H. Shih, *Phys. Rev. Lett.* **74**, 3600 (1996).
- [14] C. H. Monken, P. H. S. Ribeiro, and S. Pádua, *Phys. Rev. A* **57**, 3123 (1998).
- [15] D. Greenberger, M. A. Horne, and A. Zeilinger, *Phys. Today* **46** (8), 22 (1993).
- [16] J. D. Franson, *Phys. Rev. Lett.* **62**, 2205 (1989).
- [17] Z. Y. Ou, X. Y. Zou, L. J. Wang, and L. Mandel, *Phys. Rev. Lett.* **65**, 321 (1990).
- [18] P. G. Kwiat *et al.*, *Phys. Rev. A* **41**, 2910 (1990).
- [19] P. G. Kwiat and R. Y. Chiao, *Phys. Rev. Lett.* **66**, 588 (1991).
- [20] J. G. Rarity and P. R. Tapster, *Phys. Rev. Lett.* **64**, 2495 (1990).
- [21] L. Mandel and E. Wolf, *Optical Coherence and Quantum Optics* (Cambridge University Press, Cambridge, England, 1995).
- [22] Z. Y. Ou, *Phys. Rev. A* **37**, 1607 (1988).